

## Reversibly pH-Responsive Nanoporous Layer-by-Layer Microtubes

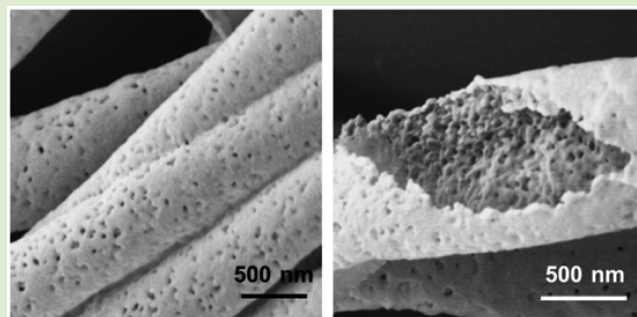
Choonghyun Sung,<sup>†</sup> Yixin Ye,<sup>‡</sup> and Jodie L. Lutkenhaus<sup>\*,†</sup>

<sup>†</sup>Artie McFerrin Department of Chemical Engineering, Texas A&M University, College Station, Texas 77843, United States

<sup>‡</sup>Department of Chemical Engineering, Tsinghua University, Beijing, People's Republic of China

### Supporting Information

**ABSTRACT:** Nanoporous layer-by-layer (LbL) microtubes consisting of poly(allylamine hydrochloride) (PAH) and poly(acrylic acid) (PAA) are prepared by LbL deposition in porous templates followed by postassembly acid treatment. The formation of the nanoporous structure is studied as a function of solution pH, treatment time, and number of layers. Pore formation is most effective at pH 1.8, requiring only 5 min to achieve a complete transition, and is shown to be reversible. Whereas the inner surface of the porous microtubes is rough, the outer surface is smoother and exhibited isolated pores, suggestive of an asymmetric porous structure.



The layer-by-layer (LbL) assembly technique is a simple technique to build up polyelectrolyte multilayers from the alternate adsorption of oppositely charged polymers (or complementary species).<sup>1–3</sup> The total film thickness can be easily controlled from nano- to microscale by the number of deposition cycles or assembly parameters (ionic strength, pH, etc.).

Recently, porous planar LbL films have been proposed for applications such as superhydrophobic coatings,<sup>4</sup> antireflection films,<sup>5</sup> Bragg reflectors,<sup>6</sup> and drug delivery.<sup>7</sup> Porosity is generated in the LbL film using postassembly immersion in acidic or basic solution. When LbL films of weak polyelectrolytes, poly(allylamine hydrochloride) (PAH) and poly(acrylic acid) (PAA), are immersed in acidic solution and then rinsed in deionized water, nano- or micropores are formed.<sup>5,8</sup> Elsewhere, treatment of hydrogen-bonded LbL films of poly(4-vinylpyridine) (PVP) and PAA in pH 12.5 solution generates micropores.<sup>9,10</sup> Porous LbL films can be also be obtained from sacrificial porous templates (e.g., CaCO<sub>3</sub>).<sup>11–13</sup>

The formation of pores in PAH/PAA LbL films by the sequential exposure to acid and then water has been explained in terms of macroscopic restructuring.<sup>14</sup> During immersion in acidic solution, the LbL film swells as a result of carboxylic acid protonation and subsequent breakage of ion pairs. Consequent immersion in slightly higher pH water allows ion pairs to reform along with rejection of water from the film, causing the formation of small water pockets. Porous films are obtained when these water pockets are emptied via drying. In contrast, pore formation in hydrogen-bonded PVP/PAA LbL films is attributed to the removal of PAA followed by the restructuring of PVP on the supporting substrate.<sup>9</sup>

In addition to porous films, porous nanotubes and microtubes have attracted great interest. For example, porous metallic or metal oxide nanotubes have been explored for various applications such as energy,<sup>15,16</sup> sensing,<sup>17,18</sup> and

photocatalysis.<sup>19</sup> Porous microtubes and nanotubes are of interest because they offer a hierarchical surface; large micron-scale features result from the tubes themselves, whereas small nanoscale features arise from the textured tube's surface. Porous platinum microtubes demonstrated improved electrocatalytic activity for proton exchange membrane fuel cells.<sup>20</sup> It was suggested that the high activity arose from the high surface-to-volume ratio, which enhanced accessibility throughout the porous structure.

Nonporous LbL nanotubes and microtubes can be easily prepared using porous membranes as a sacrificial template.<sup>21</sup> Proposed applications have ranged from biomedical to energy areas.<sup>22,23</sup> With a few noted exceptions,<sup>14,24</sup> the porous transition has largely been restricted to planar LbL films. Further, there is limited knowledge regarding the preparation of porous LbL microtubes and their controlling factors. Tian et al. demonstrated the formation of pores in hydrogen-bonded LbL microtubes consisting of PVP and PAA.<sup>24</sup> However, hydrogen-bonded LbL assemblies tend to be less stable over a broad range of pH, and the PVP/PAA porous transition was not reversible. Recently, PAH/PAA LbL microtubes with micron-scale periodic perforations were demonstrated by incubation in high-temperature aqueous media.<sup>25</sup> However, the size of perforations was very large (1.5 μm) compared to the microtube dimension (1 μm diameter and 10 μm length) and smaller nanosized pores were not achieved.

Accordingly, we hypothesized that the porous transition for PAH/PAA LbL microtubes could be leveraged to realize microtubes capable of reversible switching between nanoporous and nonporous states. Prior work by Chia et al. has shown the reversible swelling of PAH/PAA hydrated microtube arrays,

Received: January 31, 2015

Accepted: March 11, 2015

Published: March 13, 2015

which is suggestive of a bulk-scale rearrangement of the structure.<sup>14</sup> Therefore, we chose to investigate PAH/PAA microtubes in the dry state to assess whether or not nanopores form, under what conditions do the nanopores form, and whether or not the transition is reversible.

LbL films were assembled on track-etched polycarbonate (PC) membranes at pH 7.5 and 3.5 for PAH and PAA, respectively (Figure 1). Excess film on the membrane's face was

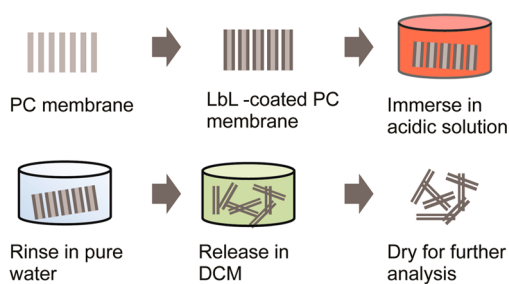


**Figure 1.** LbL assembly is conducted on a polycarbonate (PC) membrane. The LbL-coated PC membrane is then immersed in acidic solution of varying pH and rinsed briefly in water to induce the formation of nanopores. The PC membrane is then selectively removed using dichloromethane (DCM) to obtain nanoporous microtubes.

removed using oxygen plasma treatment. As a result, the LbL film coated only the interior pore walls of the PC membrane. To generate nanopores, the LbL-coated PC membrane was immersed in acidic solution followed by three separate rinses in Milli-Q 18.2 MΩ·cm water with gentle agitation. Unless stated otherwise, 21 layers were deposited, immersion time in acidic solution was 5 min, and rinsing time was 2, 1, and 1 min. Lastly, the LbL microtubes were released by selective removal of the membrane using dichloromethane. Isolated microtubes were cast and dried for the further analysis.

The effect of the acidic solution's pH on the porous structure was studied using scanning and transmission electron microscopies (SEM and TEM, respectively), Figure 2. For pH 1.8 solution, pore formation was prominent, in which isolated pores of  $80 \pm 10$  nm diameter were distributed on the

microtube's outer surface, Figure 2a. In contrast, the inner wall exhibited a very rough surface morphology with pores of  $46 \pm 4$  nm diameter, Figure 2a, inset. It is possible that the pores interconnect through the wall. As the acidic solution's pH increased, the occurrence of pores on the outer surface decreased, Figure 2b–d. Also, the microtube surface appeared rougher compared to as-made LbL microtubes without acid treatment, Figure S1.

The porous structure was also confirmed via TEM. A cracked bark-like image, presumably indicative of porous structure, is shown in Figure 2e. The feature size was roughly  $90 \pm 10$  nm. The wall thickness, estimated from the contrast along the microtube's edges was about 120 nm. Despite the formation of pores, the length ( $\sim 10 \mu\text{m}$ ) and outer diameter ( $0.9\text{--}1 \mu\text{m}$ ) of the treated microtubes were comparable to that of the original PC membrane pores. The TEM features looked largely the same for all acidic solution pH's except for pH 2.4, for which the bark-like features were less prominent and less frequently observed.

Considering the SEM and TEM images for the pH 1.8 condition, Figure 2a,e, the microtube wall possibly has a gradient or asymmetric porous structure. The pore size (40–50 nm) at the inner tube wall was slightly smaller than the pore size (60–90 nm) at the outer wall. Feature sizes ( $\sim 90$  nm) obtained from TEM images were consistent in scale with features observed at the outer wall. It is interesting that fewer pores appear on the surface. Possibly, restructuring of the LbL film was restricted at the outer wall because of strong interactions with the membrane pore wall. For this reason, the interior of the LbL microtube, having first contact with the acidic solution, was more responsive to the porous transition.

Gradient or asymmetric porous structures have been reported previously for planar LbL films of linear polyethylene imine (LPEI) and PAA treated in pH 2.0 solution.<sup>26</sup> The pores near the substrate were significantly larger than those near the film surface. The authors postulated that nanopores were quickly formed at the film's surface, while the formation of pores inside the film was slower, leading to the larger micropores at the interior. Alternatively, Cho et al. suggested that the structure of the original film is different near the

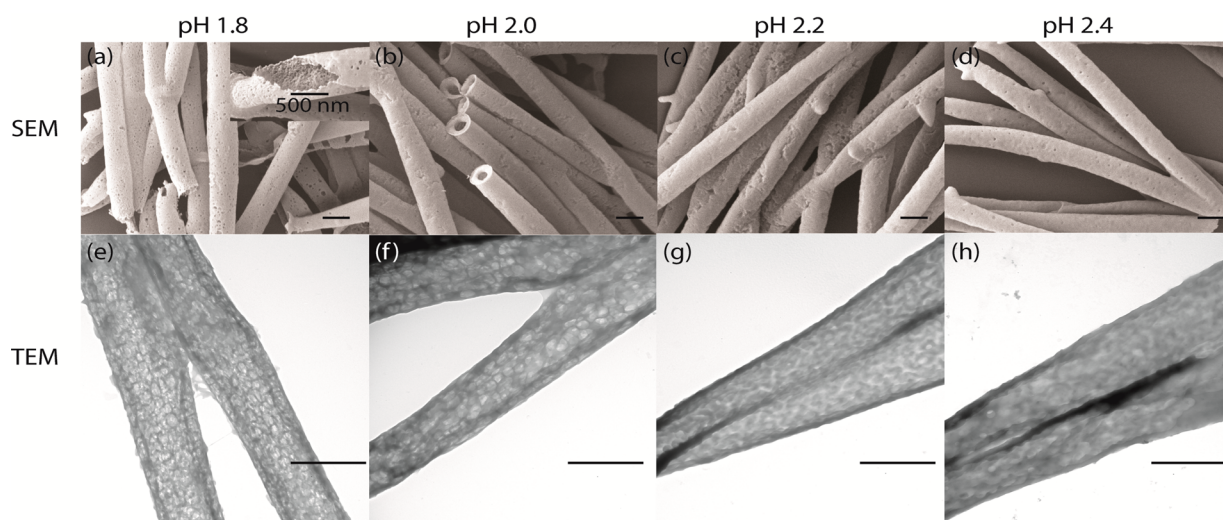


**Figure 2.** SEM (a–d) and TEM (e–h) images of LbL microtubes that had been immersed in acidic solution followed by rinsing in water. The scale bar is 1  $\mu\text{m}$  except for the inset of (a). Acidic treatment at pH 1.8 (a, e), pH 2.0 (b, f), pH 2.2 (c, g), pH 2.4 (d, h).

substrate versus the free surface, causing heterogeneity in pore size upon postassembly treatment.<sup>27</sup>

The nature of the pores formed in the LbL microtubes was compared to that in planar LbL films for pH 1.8 and 2.4 postassembly conditions. At pH 1.8, both planar LbL films and the interior wall of LbL microtubes showed a rough surface with features less than 50 nm in size, Figure 2a versus Figure S2a. In contrast, at pH 2.4, planar LbL films showed larger pores (30–800 nm diameter), whereas the comparable LbL microtubes only showed weak evidence of pore formation Figure 2d versus Figure S2b.

It has been reported in planar LbL films that pore formation is effective below pH 2.5, which coincides with the effective  $pK_a$  of PAA in planar LbL films.<sup>8</sup> As one departs from the  $pK_a$  of PAA, the driving force for pore formation increases. Considering that pore formation in LbL microtubes is less effective at pH 2.4, the  $pK_a$  of PAA within the microtubes might be near 2.4, consistent with the value found in ref 8. Another possible explanation for weak pore formation at pH 2.4 is that attractive interactions between the LbL microtube and the template's are stronger than the driving interactions for pore formation, which are weak when the pH of the acid solution is close to the  $pK_a$  of PAA.

The effect of postassembly treatment time on pore formation in LbL microtubes was investigated as well. Figure 3a–d shows SEM images of microtubes treated for varying acid-treatment times, while the pH (1.8) and subsequent water rinse time (4 min) were kept constant. Pores became clearly visible on the microtube surface after 5 min of acid treatment. The size and occurrence of the pores on the outer wall do not appear to change much with longer acid treatment times. In Figure 3e,f,

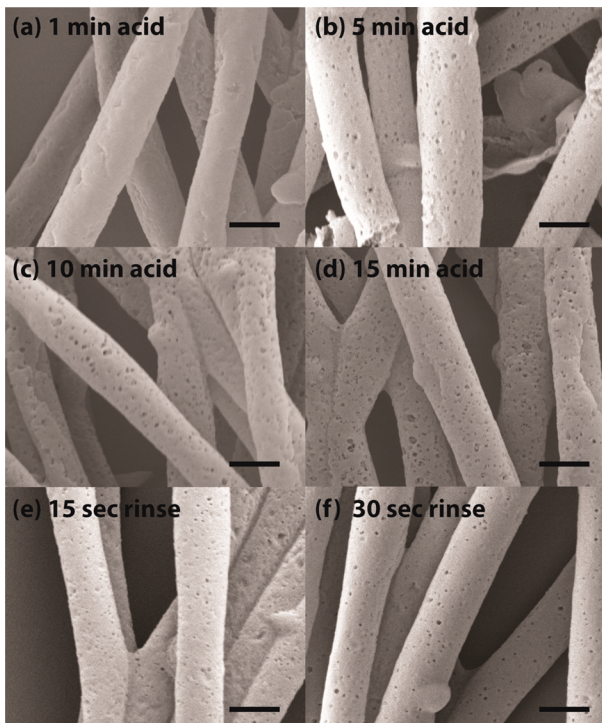


**Figure 3.** SEM images of LbL microtubes acid-treated at pH 1.8 for (a) 1, (b) 5, (c) 10, and (d) 15 min, followed by rinsing in water for 4 min. LbL microtubes treated in acid-treated at pH 1.8 for 5 min followed by rinsing in water for (e) 15 and (f) 30 s. The scale bar is 1  $\mu$ m.

the acid treatment time (5 min) and pH (1.8) were kept constant, and the water rinse time was varied. When the water rinsing time was less than 1 min, smaller pores occur. It is probable that there is not sufficient time for water to diffuse through the tube wall to complete the porous transition for these short water-rinsing times.

For comparison, planar LbL films briefly exposed to acidic solution (pH 1.8, 1 min) and briefly rinsed with water (15 s) exhibited a well-developed porous structure, Figure S3a. However, in the case of LbL microtubes, no signs of pores were observed when treated at equivalent conditions, Figure S3b. This result supports the idea that interactions between the LbL microtube and the template pore wall slow the kinetics of pore formation relative to an analogous planar LbL film.

The effect of the number of layers of polyelectrolytes on the pore formation was studied, Figure 4. Below 21 layers (or 10.5

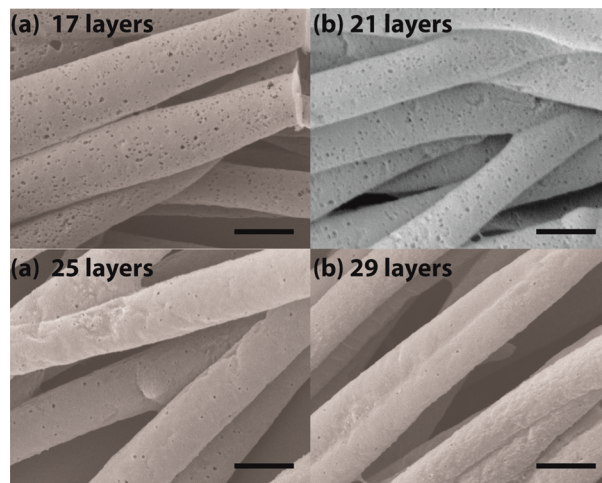


**Figure 4.** SEM images of acid-treated LbL microtubes consisting of (a) 17, (b) 21, (c) 25, and (d) 29 layers. The scale bar is 1  $\mu$ m. Below 21 layer pairs, pores were formed within the 5 min treatment time. Above 25 layer pairs, no pores were observed from similar conditions.

layer pairs), the pores were clearly observed, but above 25 layers (12.5 layer pairs), the pores on the microtube surface were absent. This result can be interpreted in the same context as the effect of acid treatment time. At 25 layers, the tube wall is thick and requires more time to undergo the porous transition, and 5 min of acid-treatment time is no longer sufficient. Beyond 25 layers, assembly within the pore became impossible because of clogging at the pore's mouth, thus, restricting our investigation for thicker tube walls, Figure S4. We attempted to plasma etch the clogged membranes to reopen the pores, but etching proved unsuccessful.

The reversibility of the porous transition was investigated, Figure 5. The reversible generation and erasure of the porous structure in planar PAH/PAA LbL films has been previously reported,<sup>5,14</sup> so we hypothesized that the LbL microtubes formed here might possess reversibility as well. The LbL-coated membranes were cycled between the pH 1.8 acid solution and rinsing water. After the given cycle, the membranes were dried and microtubes were released. The microtubes exhibited pores after the rinsing step, and microtubes became nonporous after the acid-treatment step. This supports the idea that the formation of pores is linked to the swelling and deswelling of LbL films arising from protonation and deprotonation of PAA acid groups.<sup>14</sup> Interestingly, microtubes dried from acidic

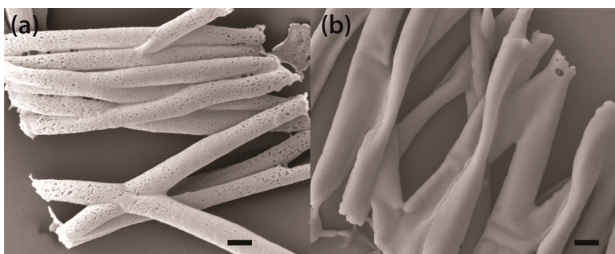


**Figure 5.** SEM images of LbL microtubes cycled between pH 1.8 acid solution and water as noted (a) acid/water/acid/water and (b) acid/water/acid/water steps. The scale bar represents 1  $\mu\text{m}$ .

solution collapsed and flattened, whereas microtubes dried from water retained their tubular structure without collapsing. This result is consistent with planar analogs, in which the LbL assembly becomes softer due to the disruption of ion pairs during acid treatment.<sup>8,14</sup> Others have suggested that repeated acid treatments result in a loss of material from the LbL assembly.<sup>8,9,27</sup> Should this be the case, one would expect the microtubes to gradually lose their reversibility or original overall shape. Here, reversibility was retained over two cycles, so we concluded that if mass is lost during the process, it is not substantial so as to affect the porous transition.

The porous transition showed good reversibility so long as the microtubes are dried following the sequential steps of acid treatment and water rinsing. We found that once dried, the tubes could not be retreated with acid or water to obtain a porous structure. Instead the reconstituted microtubes broke or deformed severely, Figure S5. This result demonstrates that the reversible porous transition is best utilized in aqueous conditions without drying in between steps.

In summary, nanoporous PAH/PAA LbL microtubes were demonstrated for the first time by postassembly acid treatment. The acid treatment pH, time, and number of layers influenced pore formation. The porous structure appears to be symmetric with small pores located at the interior pore wall and slightly larger pores at the outer pore wall, which is possibly a result of interactions between the LbL assembly and the template wall. The transition proved to be reversible so long as the tubes were dried only for observation. This finding points to the possibility of using these textured microtubes as templates themselves for hierarchical nanostructures where high surface-to-volume is desired.

## ■ ASSOCIATED CONTENT

### Supporting Information

Materials and method; SEM and TEM images of as-made PAH/PAA LbL microtubes; AFM images of planar LbL films after acid treatment; AFM image of planar LbL film and SEM image of LbL microtubes treated in pH 1.8 for short treatment time; SEM images of acid-treated LbL microtubes of varying numbers of layers. This material is available free of charge via the Internet at <http://pubs.acs.org>.

## ■ AUTHOR INFORMATION

### Corresponding Author

\*Phone: 979-845-2682. E-mail: jodie.lutkenhaus@tamu.edu.

### Notes

The authors declare no competing financial interest.

## ■ ACKNOWLEDGMENTS

This material is based on work supported by the National Science Foundation under Grant No. 1049706.

## ■ REFERENCES

- (1) Decher, G. *Science* **1997**, *277*, 1232–1237.
- (2) Ariga, K.; Hill, J. P.; Ji, Q. M. *Phys. Chem. Chem. Phys.* **2007**, *9*, 2319–2340.
- (3) Boudou, T.; Crouzier, T.; Ren, K. F.; Blin, G.; Picart, C. *Adv. Mater.* **2010**, *22*, 441–467.
- (4) Zhai, L.; Cebeci, F. C.; Cohen, R. E.; Rubner, M. F. *Nano Lett.* **2004**, *4*, 1349–1353.
- (5) Hiller, J.; Mendelsohn, J. D.; Rubner, M. F. *Nat. Mater.* **2002**, *1*, 59–63.
- (6) Zhai, L.; Nolte, A. J.; Cohen, R. E.; Rubner, M. F. *Macromolecules* **2004**, *37*, 6113–6123.
- (7) Berg, M. C.; Zhai, L.; Cohen, R. E.; Rubner, M. F. *Biomacromolecules* **2006**, *7*, 357–364.
- (8) Mendelsohn, J. D.; Barrett, C. J.; Chan, V. V.; Pal, A. J.; Mayes, A. M.; Rubner, M. F. *Langmuir* **2000**, *16*, 5017–5023.
- (9) Fu, Y.; Bai, S. L.; Cui, S. X.; Qiu, D. L.; Wang, Z. Q.; Zhang, X. *Macromolecules* **2002**, *35*, 9451–9458.
- (10) Bai, S. L.; Wang, Z. Q.; Zhang, X.; Wang, B. *Langmuir* **2004**, *20*, 11828–11832.
- (11) Sukhorukov, G. B.; Volodkin, D. V.; Gunther, A. M.; Petrov, A. I.; Shenoy, D. B.; Mohwald, H. *J. Mater. Chem.* **2004**, *14*, 2073–2081.
- (12) Volodkin, D. V.; Larionova, N. I.; Sukhorukov, G. B. *Biomacromolecules* **2004**, *5*, 1962–1972.
- (13) Kozlovskaya, V.; Chen, J.; Tedjo, C.; Liang, X.; Campos-Gomez, J.; Oh, J.; Saeed, M.; Lungu, C. T.; Kharlampieva, E. *J. Mater. Chem. B* **2014**, *2*, 2494–2507.
- (14) Chia, K. K.; Rubner, M. F.; Cohen, R. E. *Langmuir* **2009**, *25*, 14044–14052.
- (15) Du, N.; Zhang, H.; Chen, B.; Wu, J. B.; Ma, X. Y.; Liu, Z. H.; Zhang, Y. Q.; Yang, D.; Huang, X. H.; Tu, J. P. *Adv. Mater.* **2007**, *19*, 4505–.
- (16) Cao, F.; Pan, G. X.; Xia, X. H.; Tang, P. S.; Chen, H. F. *J. Power Sources* **2014**, *264*, 161–167.
- (17) Giri, A. K.; Sinhamahapatra, A.; Prakash, S.; Chaudhari, J.; Shahi, V. K.; Panda, A. B. *J. Mater. Chem. A* **2013**, *1*, 814–822.
- (18) Du, N.; Zhang, H.; Chen, B. D.; Ma, X. Y.; Liu, Z. H.; Wu, J. B.; Yang, D. R. *Adv. Mater.* **2007**, *19*, 1641.
- (19) Hua, X.; Jin, Y. J.; Wang, K.; Li, N.; Liu, H. Q.; Chen, M. D.; Paul, S.; Zhang, Y.; Zhao, X. D.; Teng, F. *Catal. Commun.* **2014**, *52*, 49–52.
- (20) Zhao, P.; Ragam, S.; Ding, Y. J.; Zotova, I. B.; Mu, X.; Lee, H.-C.; Meissner, S. K.; Meissner, H. *Opt. Lett.* **2012**, *37*, 1283–1285.
- (21) Wang, Y.; Angelatos, A. S.; Caruso, F. *Chem. Mater.* **2008**, *20*, 848–858.
- (22) He, Q.; Cui, Y.; Ai, S. F.; Tian, Y.; Li, J. B. *Curr. Opin. Colloid Interface Sci.* **2009**, *14*, 115–125.
- (23) Azzaroni, O.; Lau, K. H. A. *Soft Matter* **2011**, *7*, 8709–8724.
- (24) Tian, Y.; He, Q.; Cui, Y.; Tao, C.; Li, J. B. *Chem.—Eur. J.* **2006**, *12*, 4808–4812.
- (25) Sung, C.; Vidyasagar, A.; Hearn, K.; Lutkenhaus, J. L. *J. Mater. Chem. B* **2014**, *2*, 2088–2092.
- (26) Lutkenhaus, J. L.; McEnnis, K.; Hammond, P. T. *Macromolecules* **2008**, *41*, 6047–6054.
- (27) Cho, C.; Jeon, J. W.; Lutkenhaus, J.; Zacharia, N. S. *ACS Appl. Mater. Interfaces* **2013**, *5*, 4930–4936.